

54-65
N89-16752

VON KARMAN INSTITUTE FOR FLUID DYNAMICS

LECTURE SERIES 1988-04

INTAKE AERODYNAMICS

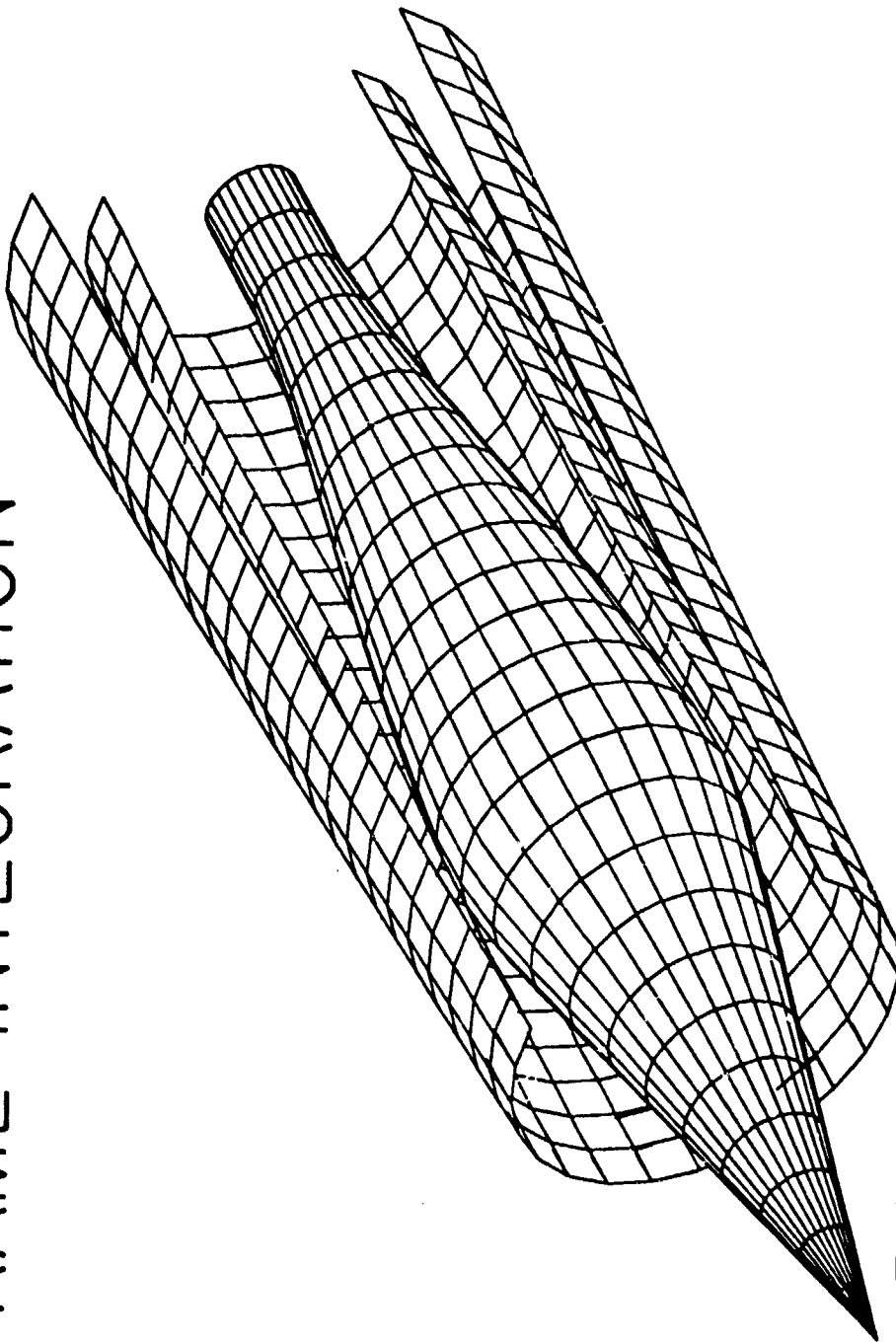
FEBRUARY 22 - 26, 1988

COMPUTATIONAL METHODS FOR INLET AIRFRAME INTEGRATION

Charles E. Towne

NASA-Lewis Research Center, Ohio, USA

COMPUTATIONAL METHODS FOR INLET AIRFRAME INTEGRATION



Charles E. Towne
Senior Research Engineer
NASA Lewis Research Center - Cleveland Ohio - USA

OUTLINE

Interest in the use of computational fluid dynamics (CFD) for the design and analysis of aircraft intakes has increased greatly in the past few years. Several factors have contributed to this growth, including: (1) complex geometric design requirements for many modern propulsion systems, leading to flow phenomena that may not be intuitively predictable; (2) increasing fuel costs, leading to potentially large cost savings for even small performance improvements; (3) the high cost of extensive experimental testing; (4) the continued development and improvement of sophisticated numerical algorithms for solving the complex equations governing fluid flow; and (5) the increasing availability of supercomputers.

Many different computational methods have been and continue to be used for studying internal flow. To effectively utilize these computational tools, today's inlet designer must be aware of the types of methods are applicable to a specific problem, and of their capabilities and limitations.

The object of this presentation, therefore, is to remove some of the mystery from CFD by systematically discussing the basic types of analyses commonly used for internal flows. While the numerical algorithms used to solve the governing equations are important and will be mentioned, they will not be discussed in detail. Instead, for each type of analysis the emphasis will be on the simplifying assumptions made to the fundamental, or Navier-Stokes equations, and the resulting advantages and disadvantages. Examples of computed results will be shown for each type of analysis. The talk will conclude with a summary of the current overall status of CFD in propulsion research.

OUTLINE

- FUNDAMENTAL EQUATIONS
- ANALYSES USED FOR INTERNAL FLOW
 - IRRATIONAL
 - EULER
 - BOUNDARY LAYER
 - PARABOLIZED NAVIER-STOKES
 - TIME-AVERAGED NAVIER-STOKES
- ASSUMPTIONS MADE
- SOLUTION METHODS
 - +'S AND -'S
 - EXAMPLES
- OVERALL STATUS OF CFD IN PROPULSION

FUNDAMENTAL EQUATIONS

These equations are simply the basic conservation laws, in differential form, for mass, momentum, and energy. For simplicity, they have been written in a 2-D Cartesian coordinate system. They are in what is called conservation form, and have been non-dimensionalized by appropriate reference quantities. In order, they are commonly called the continuity, x-momentum, y-momentum, and energy equations. Several different versions of the energy equation appear in the literature. Two of the most common ones are shown here, with total energy and total enthalpy as the dependent variables.

Although, strictly speaking, the term "Navier-Stokes" applies only to the two momentum equations, all four equations as a set are generally referred to as the Navier-Stokes equations. Together with the auxiliary equations and definitions shown in the next figure, they completely describe the motion of any continuum flow of a Newtonian fluid. (Body forces and internal heat addition have been assumed negligible. However, these terms could also be included). Turbulence can also be computed with these equations. With current and foreseeable computers, however, it's not feasible to resolve the small time and length scales required to actually compute turbulence for realistic propulsion system problems. Turbulence is therefore modeled using various assumptions. With the turbulence models used for practical engineering problems, the viscosity and thermal conductivity coefficients are locally increased to account for the increased diffusion due to turbulence. They are then known as "effective" viscosity and thermal conductivity coefficients. The result is that the Navier-Stokes equations normally used for turbulent flow look exactly like the ones shown here.

These equations are a coupled set of nonlinear second-order partial differential equations, and are therefore very difficult to solve. Closed form solutions exist only for a few very simplified cases. To solve more realistic fluid flow problems, assumptions are usually made about the flow that allow these equations to be simplified.

FUNDAMENTAL EQUATIONS NAVIER-STOKES EQUATIONS

$$\begin{aligned} \frac{\partial \rho}{\partial t} + \frac{\partial(\rho u)}{\partial x} + \frac{\partial(\rho v)}{\partial y} &= 0 \\ \frac{\partial(\rho u)}{\partial t} + \frac{\partial(\rho u^2)}{\partial x} + \frac{\partial(\rho uv)}{\partial y} - \frac{\partial p}{\partial x} + \frac{1}{Re} \left(\frac{\partial \tau_{xx}}{\partial x} + \frac{\partial \tau_{xy}}{\partial y} \right) &= 0 \\ \frac{\partial(\rho v)}{\partial t} + \frac{\partial(\rho uv)}{\partial x} + \frac{\partial(\rho v^2)}{\partial y} - \frac{\partial p}{\partial y} + \frac{1}{Re} \left(\frac{\partial \tau_{xy}}{\partial x} + \frac{\partial \tau_{yy}}{\partial y} \right) &= 0 \\ \frac{\partial(\rho E_T)}{\partial t} + \frac{\partial(u E_T)}{\partial x} + \frac{\partial(v E_T)}{\partial y} - \frac{\partial(u p)}{\partial x} - \frac{\partial(v p)}{\partial y} - \frac{1}{Re P_T} \left(\frac{\partial q_x}{\partial x} + \frac{\partial q_y}{\partial y} \right) &= 0 \\ + \frac{1}{Re} \left[\frac{\partial}{\partial x} (u \tau_{xx} + v \tau_{xy}) + \frac{\partial}{\partial y} (u \tau_{xy} + v \tau_{yy}) \right] &- \partial \dot{E} = 0 \\ \frac{\partial(\rho H)}{\partial t} + \frac{\partial(\rho u H)}{\partial x} + \frac{\partial(\rho v H)}{\partial y} - \frac{1}{Re F_T} \left(\frac{\partial q_x}{\partial x} + \frac{\partial q_y}{\partial y} \right) &= 0 \\ + \frac{1}{Re} \left[\frac{\partial}{\partial x} (u \tau_{xx} + v \tau_{xy}) + \frac{\partial}{\partial y} (u \tau_{xy} + v \tau_{yy}) \right] & \end{aligned}$$

FUNDAMENTAL EQUATIONS AUXILIARY EQUATIONS

$$\begin{aligned} p &= \rho R T \\ \tau_{xx} &= 2\mu \frac{\partial u}{\partial x} + \lambda \left(\frac{\partial u}{\partial x} + \frac{\partial v}{\partial y} \right) \\ \tau_{yy} &= 2\mu \frac{\partial v}{\partial y} + \lambda \left(\frac{\partial u}{\partial x} + \frac{\partial v}{\partial y} \right) \\ \tau_{xy} &= \mu \left(\frac{\partial u}{\partial x} + \frac{\partial v}{\partial y} \right) \\ q_x &= -k \frac{\partial T}{\partial x} \\ q_y &= -k \frac{\partial T}{\partial y} \\ E_T &= \rho c_v T + \frac{1}{2} \rho (u^2 + v^2) \\ H &= c_p T + \frac{1}{2} (u^2 + v^2) \end{aligned}$$

POTENTIAL FLOW ANALYSES - BASIC ASSUMPTIONS

Potential flow analyses are among the oldest and most well established methods currently being used for internal flow. The flow is assumed to be irrotational (i.e., the curl of the velocity vector, or the vorticity, is assumed to be zero). Since viscosity introduces vorticity into the flow, this implies the flow is inviscid. The flow is also assumed to be steady and isentropic.

POTENTIAL FLOW ANALYSES BASIC ASSUMPTIONS

- IRROTATIONAL ($\nabla \times \vec{V} = 0$)
- INVISCID
- STEADY & ISENTROPIC

POTENTIAL FLOW ANALYSES - BASIC ASSUMPTIONS

This figure relates the basic assumptions for potential flow to the terms in the Navier-Stokes equations. All the viscous and heat conduction terms are eliminated. They are therefore most valid at high Reynolds numbers. The key assumption, however, is irrotationality. Mathematically, since the curl of the velocity vector is zero, the velocity can be expressed as the gradient of a scalar. This scalar, ϕ , is called the velocity potential.

POTENTIAL FLOW ANALYSES BASIC ASSUMPTIONS

$$\begin{aligned}
 \frac{\partial(\rho u)}{\partial x} + \frac{\partial(\rho v)}{\partial y} &= 0 \\
 \frac{\partial(\rho u^2)}{\partial x} + \frac{\partial(\rho uv)}{\partial y} &= -\frac{\partial p}{\partial x} + \frac{1}{Re} \left(\frac{\partial \tau_{xx}}{\partial x} + \frac{\partial \tau_{xy}}{\partial y} \right) \\
 \frac{\partial(\rho uv)}{\partial x} + \frac{\partial(\rho v^2)}{\partial y} &= -\frac{\partial p}{\partial y} + \frac{1}{Re} \left(\frac{\partial \tau_{xy}}{\partial x} + \frac{\partial \tau_{yy}}{\partial y} \right) \\
 \frac{\partial(uE_T)}{\partial x} + \frac{\partial(vE_T)}{\partial y} &= -\frac{\partial(up)}{\partial x} - \frac{\partial(vp)}{\partial y} - \frac{1}{RePr} \left(\frac{\partial q_x}{\partial x} + \frac{\partial q_y}{\partial y} \right) \\
 &\quad + \frac{1}{Re} \left[\frac{\partial}{\partial x} (u\tau_{xx} + v\tau_{xy}) + \frac{\partial}{\partial y} (u\tau_{xy} + v\tau_{yy}) \right]
 \end{aligned}$$

$$\nabla \times \vec{V} = 0 \quad \rightarrow \quad \nabla \phi = \vec{V}$$

POTENTIAL FLOW ANALYSES - GOVERNING EQUATIONS

The irrotationality condition allows the velocity field to be described by a single equation for the velocity potential ϕ . For compressible flow this equation is called the full potential equation and is derived using the continuity equation, the momentum equations, and the definition of the speed of sound a . This is a nonlinear second-order partial differential equation. If the speed of sound approaches infinity (incompressible flow), this equation reduces to Laplace's equation, which is still second-order, but linear. After solving for the velocity potential (and hence the velocity field itself), pressure, temperature, etc., can be computed from the momentum and energy equations.

A few words should be said about the mathematical character of the potential flow equation. (This also applies to the Euler equations to be discussed later). For subsonic flow, the equation is elliptic. This means that the solution at a point depends on the conditions at all the boundaries of the flow domain, including the downstream boundary. For supersonic flow however, the equation is hyperbolic, and the solution at a point depends only on the upstream conditions.

POTENTIAL FLOW ANALYSES GOVERNING EQUATIONS

- COMPRESSIBLE FLOW

$$\left[1 - \frac{1}{a^2} \left(\frac{\partial \phi}{\partial x} \right)^2 \right] \frac{\partial^2 \phi}{\partial x^2} + \left[1 - \frac{1}{a^2} \left(\frac{\partial \phi}{\partial y} \right)^2 \right] \frac{\partial^2 \phi}{\partial y^2} - \frac{2}{a^2} \frac{\partial \phi}{\partial x} \frac{\partial \phi}{\partial y} \frac{\partial^2 \phi}{\partial x \partial y} = 0$$

- INCOMPRESSIBLE FLOW

$$\frac{\partial^2 \phi}{\partial x^2} + \frac{\partial^2 \phi}{\partial y^2} = 0$$

- REMAINING VARIABLES FROM ENERGY EQUATION, MOMENTUM EQUATIONS, ETC.

- MATHEMATICAL CLASSIFICATION

- $M < 1 \rightarrow$ ELLIPTIC
- $M > 1 \rightarrow$ HYPERBOLIC

POTENTIAL FLOW ANALYSES - SOLUTION METHODS

For incompressible flows, since the governing equation is linear, complex flows can be described by superposition of solutions for simpler flows. A common procedure is to distribute a series of point sources and sinks, of properly varying strengths, along the surface of the duct. In three dimensions these procedures are generally called panel methods. The incompressible equation can also be solved using complex variable methods, in which a complex geometry is transformed into a simple geometry using conformal mapping. However, this procedure is limited to two-dimensional flows. There are also several iterative numerical techniques that have been used.

Compressible flows are sometimes computed by solving the incompressible problem and applying a compressibility correction. For slender geometries that only "slightly" perturb the uniform external flow, small perturbation methods can be used. This assumption allows the full potential equation to be linearized, and therefore more easily solved. And finally, several iterative numerical techniques have also been used for the full potential equation.

POTENTIAL FLOW ANALYSES SOLUTION METHODS

INCOMPRESSIBLE

- SUPERPOSITION OF SIMPLE FLOWS
- COMPLEX VARIABLE METHODS
- ITERATIVE NUMERICAL METHODS

COMPRESSIBLE

- INCOMPRESSIBLE WITH COMPRESSIBILITY CORRECTION
- SMALL PERTURBATION METHODS
- ITERATIVE NUMERICAL METHODS

POTENTIAL FLOW ANALYSES - +'S AND -'S

Potential flow methods have been around for many years. The mathematical theory is well understood, and the potential equation is relatively easy to solve, especially for incompressible flow. There are many computer codes available, and they are generally easy to use.

One of the disadvantages of using potential methods for internal flow is that viscous effects are often important and potential flow is, of course, inviscid. The assumption of isentropic flow means that these methods are, strictly speaking, not valid across shock waves. (However, if the Mach number normal to the shock is near one the flow is nearly isentropic). In addition, methods that solve the potential equation in non-conservation form, as presented earlier, often have trouble conserving mass (the so-called "leakage" problem).

Potential methods are most useful in subsonic or transonic flows in which the pressure distribution is of primary interest and in which viscous effects are relatively minor. They are generally cheap to use and are therefore often used in preliminary design studies that require many cases to be run. They also can be used to determine a pressure distribution for boundary layer or parabolized Navier-Stokes analyses. The full potential equation is the basis for many transonic flow analyses.

POTENTIAL FLOW ANALYSES + 'S AND - 'S

ADVANTAGES

- WELL DEVELOPED MATHEMATICAL THEORY
- INCOMPRESSIBLE FORM RELATIVELY EASY TO SOLVE
- COMPUTER CODES WIDELY AVAILABLE, EASY TO USE

DISADVANTAGES

- NO VISCOUS EFFECTS
- ISENTROPIC
- MASS FLOW LEAKAGE

AREAS OF APPLICATION

- PRELIMINARY DESIGN STUDIES
- VISCOUS/INVISCID INTERACTION
- TRANSONIC FLOW
- INLETS, NOZZLES, TURBOMACHINERY

POTENTIAL FLOW ANALYSES - EXAMPLE 1

In this figure potential flow results are presented and compared with experimental data for a three-dimensional "scoop" inlet at an angle of attack of fifty degrees. Static pressure is plotted as a function of axial distance at four circumferential locations. The flow was computed by Kao (Ref. 1) using the incompressible 3-D Panel method of Reference 2, with the compressibility correction of Reference 3. Approximately 700 panels were used to model the geometry, which included a centerbody and downstream extension not shown in the figure. The experimental data are from Reference 4.

The agreement between the potential flow results and the experimental data is generally very good. The poorest agreement is along the lower internal surface, and is probably due to boundary blockage effects and possible flow separation. These effects, of course, are not modeled by the potential flow analysis.

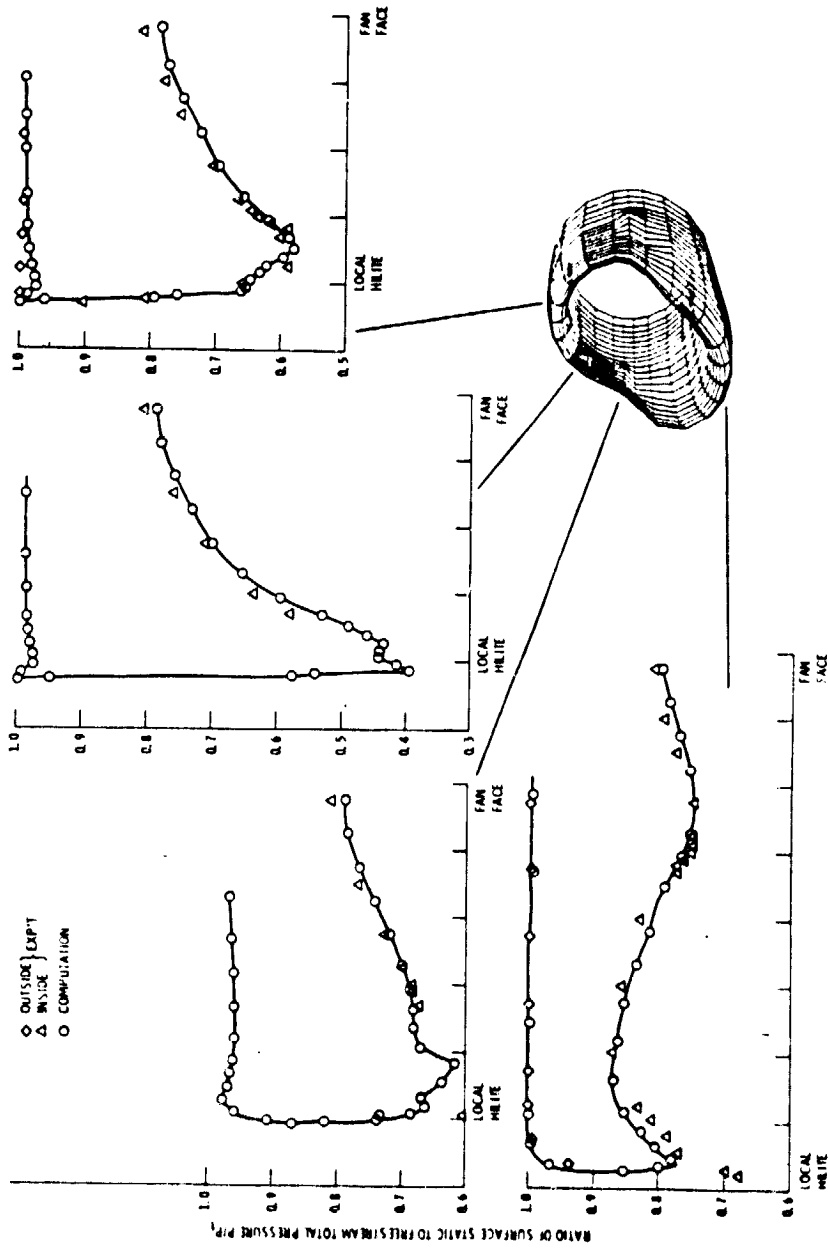


Figure 4 - Paneling and axial surface static pressure for a scoop inlet model $\alpha = 50^\circ$, $V_\infty = 41$ m/sec, $M_1 = 0.63$ (inlet Mach number).

POTENTIAL FLOW ANALYSES - EXAMPLE 2

The second potential flow example was computed by Reyhner (Ref. 5). He studied the transonic flow through a typical turbofan inlet with an asymmetric lip, as shown here. The tilt of the inlet centerline with respect to the engine centerline is intended to reduce drag by aligning the inlet with the incoming flow at cruise conditions.

Reyhner's method solves the full 3-D potential equation using an iterative successive line over-relaxation (SLOR) finite difference method. The computational grid near the inlet is shown in this figure.

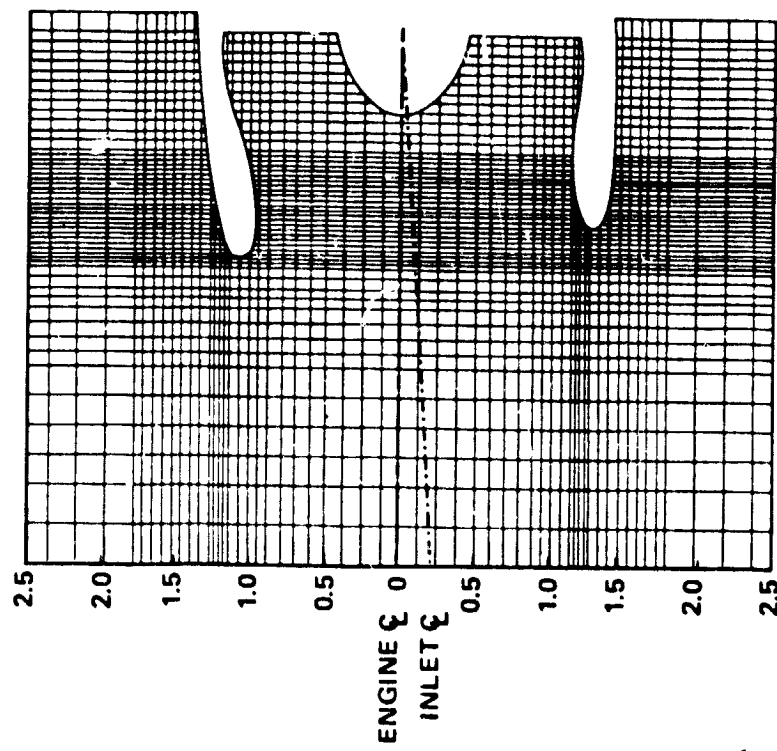


Figure 11. Computational Flowfield and Mesh in the Vicinity of a Commercial Transport Turbofan Engine Type Inlet

POTENTIAL FLOW ANALYSES - EXAMPLE 2

In this figure computed and experimental surface Mach numbers are plotted vs. axial distance at three circumferential locations. The experimental data are unpublished results from a 0.16-scale model test in the Boeing 9x9 foot low speed wind tunnel. The angle of attack was 20 degrees and the free stream velocity was 90 m/sec.

The agreement is generally very good except along the bottom (windward) surface. As in the previous example, this disagreement is believed due to blockage effects of the thickening boundary layer, which is close to separation, just inside the lower lip. (It should be noted that three other cases, with lower peak Mach numbers, were also computed and agreed more closely with experiment).

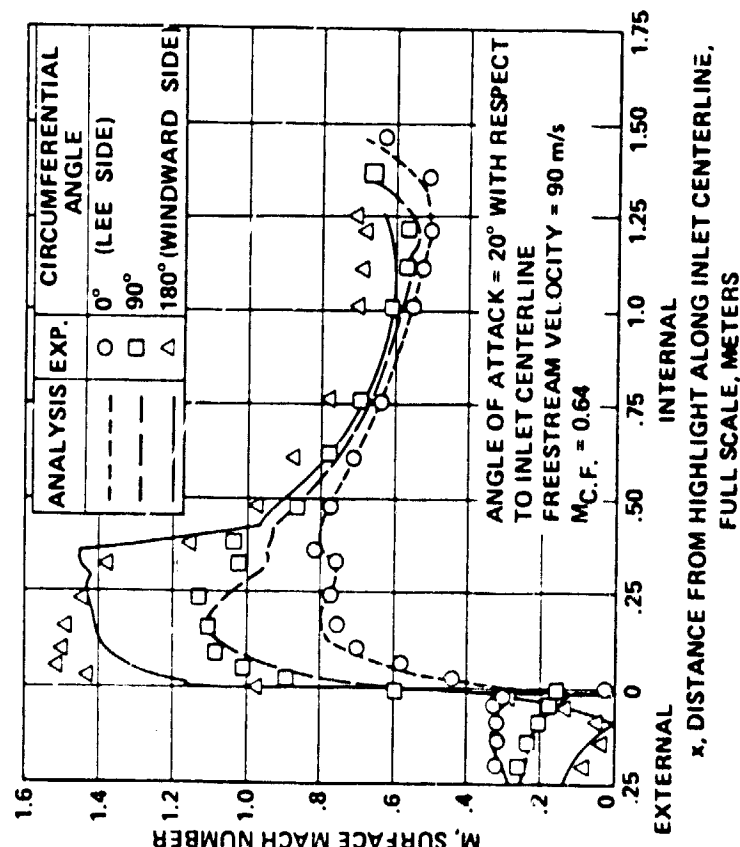


Figure 13. Cowl Surface Mach Number Distribution for an Asymmetric Commercial-Transport Turbofan-Engine Type Inlet

EULER ANALYSES - BASIC ASSUMPTIONS

Like potential flow analyses, Euler analyses are inviscid. However, unlike potential flow analyses, that is the only assumption that is made. The flow can be rotational, non-isentropic, and even unsteady.

EULER ANALYSES BASIC ASSUMPTIONS

- INVISCID

EULER ANALYSES - BASIC ASSUMPTIONS

The Euler equations are simply the Navier-Stokes equations with all the viscous and heat conduction terms eliminated. As in potential flow, they are therefore most valid at high Reynolds numbers. The equations shown are written for steady flows, but that is not a requirement. Like the Navier-Stokes equations, the Euler equations are a set of coupled nonlinear partial differential equations, but first-order instead of second-order. For steady flow, their mathematical character is the same as the potential equation - elliptic in space for subsonic flow and hyperbolic in time for supersonic flow. For unsteady flow they are hyperbolic in time.

EULER ANALYSES BASIC ASSUMPTIONS

$$\frac{\partial(\rho u)}{\partial x} + \frac{\partial(\rho v)}{\partial y} = 0$$

$$\frac{\partial(\rho u^2)}{\partial x} + \frac{\partial(\rho uu)}{\partial y} = -\frac{\partial p}{\partial x} + \frac{1}{Re} \left(\frac{\partial \tau_{xx}}{\partial x} + \frac{\partial \tau_{xy}}{\partial y} \right)$$

$$\frac{\partial(\rho vv)}{\partial x} + \frac{\partial(\rho v^2)}{\partial y} = -\frac{\partial p}{\partial y} + \frac{1}{Re} \left(\frac{\partial \tau_{xy}}{\partial x} + \frac{\partial \tau_{yy}}{\partial y} \right)$$

$$\begin{aligned} \frac{\partial(uE_T)}{\partial x} + \frac{\partial(vE_T)}{\partial y} &= -\frac{\partial(up)}{\partial x} - \frac{\partial(vp)}{\partial y} - \frac{1}{RePr} \left(\frac{\partial q_x}{\partial x} + \frac{\partial q_y}{\partial y} \right) \\ &+ \frac{1}{Re} \left[\frac{\partial}{\partial x} (u\tau_{xx} + v\tau_{xy}) + \frac{\partial}{\partial y} (u\tau_{xy} + v\tau_{yy}) \right] \end{aligned}$$

EULER ANALYSES - SOLUTION METHODS

The Euler equations are most commonly solved using finite difference techniques. For supersonic flow, the equations are hyperbolic in space and can be solved by forward marching in the streamwise direction. For subsonic flow they are elliptic in space, but hyperbolic in time. Steady subsonic (or even supersonic) flows are therefore often solved by marching the unsteady equations in time until a steady state is reached. Both explicit and implicit methods have been used. The trend seems to be toward implicit methods. These are more difficult to program and require more computer time per time step, but in theory are more stable and allow larger time steps. If only the steady-state solution is of interest, acceleration techniques are often used to speed convergence, and the results may not be time-accurate. Some researchers are using multi-grid techniques, in which a series of grids from coarse to fine are used to speed convergence to steady state. Finite element methods are used less commonly than finite difference methods, but have several strong advocates.

The method of characteristics is the most nearly exact method for numerically solving hyperbolic partial differential equations. It can be used to solve the Euler equations for steady supersonic or unsteady flow. With this method the partial differential equations reduce to ordinary differential equations along characteristic directions. The trend today, however, seems to be toward the more easily implemented finite difference methods.

EULER ANALYSES SOLUTION METHODS

- FINITE DIFFERENCE METHODS
 - SPACE MARCHING IF SUPERSONIC
 - TIME MARCHING
 - EXPLICIT OR IMPLICIT
 - MULTI-GRID TECHNIQUES
- FINITE ELEMENT METHODS
- METHOD OF CHARACTERISTICS

The Euler equations include rotational effects. For instance, if the flow entering a duct has a boundary layer-like profile, secondary flow development and even flow separation can be computed with the Euler equations. They are also valid across shock waves. With finite difference methods, shock waves are generally "captured" by the solution and smeared over a few grid points. Some form of artificial viscosity is usually required, either for stability or to eliminate oscillations. Because the flow is inviscid, there are no shear layers with large gradients to resolve and therefore fewer grid points are needed than for a Navier-Stokes solution.

For many internal flows, however, viscous effects are important and their omission may be a disadvantage. These codes can also be difficult to run because of the need to select time step size to optimize convergence, parameters controlling artificial viscosity, etc. Time dependent methods can be long running, although still faster than Navier-Stokes methods because fewer grid points are needed.

Like potential flow analyses, Euler analyses are most useful for flows in which the pressure distribution is of primary interest and in which viscous effects are relatively minor. They can be used to investigate candidate designs of propulsion system components, and to compute a pressure distribution for use by a boundary layer or parabolized Navier-Stokes analysis.

EULER ANALYSES +'S AND -'S

ADVANTAGES

- INCLUDES ROTATIONAL EFFECTS
- VALID ACROSS SHOCK WAVES
- FEWER GRID POINTS THAN NAVIER-STOKES ANALYSIS

DISADVANTAGES

- NO VISCOUS EFFECTS GENERATED
- COMPUTER CODES CAN BE DIFFICULT TO USE

AREAS OF APPLICATION

- PRELIMINARY DESIGN STUDIES
- VISCOUS/INVISCID INTERACTION
- INLETS, NOZZLES, TURBOMACHINERY

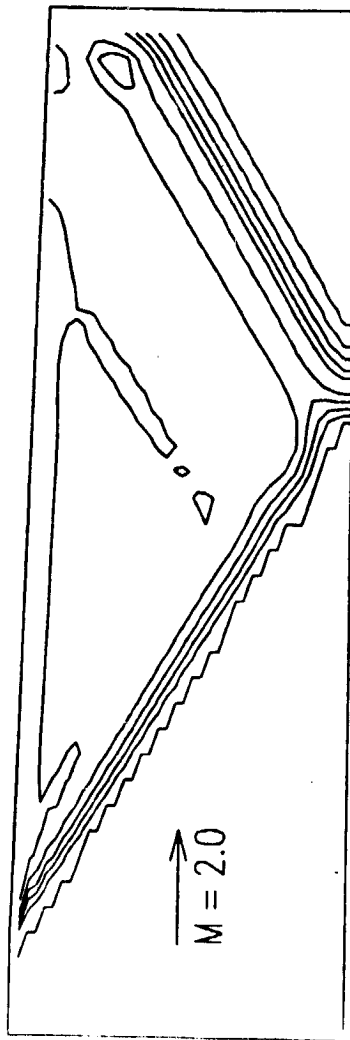
EULER ANALYSES - EXAMPLE

This figure shows Mach number contours for an oblique shock wave reflecting off a flat plate. The free stream Mach number was 2.0, and the shock was generated by a 1.6 degree wedge. (The sawtooth shape of the first contour line in the incident shock is not physical, but instead is a result of the contouring algorithm in the plotting routines).

These results were computed using PROTEUS, a user-oriented Navier-Stokes code currently under development at NASA Lewis, run in Euler mode (i.e., without the viscous terms). With this code, the unsteady governing equations are solved by marching in time using an implicit finite difference technique. A 61x61 grid was used, equally spaced in both directions, and convergence to steady state was obtained in 1200 time steps.

Since Euler methods are rotational and non-isentropic, the Rankine-Hugoniot relations are satisfied across the shock waves. Note, however, that the shocks are not sharp discontinuities but are smeared over a few grid points. They could be sharpened by using more grid points, or by packing grid points more tightly in the location of the shocks. It should also be noted that because Euler methods are inviscid, no boundary layer buildup occurs on the flat plate. The actual flow, with a shock - boundary layer interaction, would look quite different near the surface of the plate.

OBLIQUE SHOCK REFLECTION MACH NUMBER CONTOURS



BOUNDARY LAYER ANALYSES - BASIC ASSUMPTIONS

Potential and Euler analyses are inviscid. At high Reynolds numbers these analyses can yield good results for pressure distributions, but they cannot predict viscous or heat transfer effects. This limits their usefulness for internal flows, where these effects are usually important.

The oldest generalized methods to include these effects are called boundary layer methods, first developed by Prandtl in 1904. He noted that in many applications at high Reynolds numbers, viscous effects are confined to a relatively thin region near solid boundaries called the boundary layer. In deriving the boundary layer equations, the thickness of this region is assumed small relative to the size of the geometry being analyzed, and is said to be of order delta. The density, temperature, streamwise velocity, and total enthalpy, along with derivatives in the streamwise direction, are assumed to be of order 1. Gradients normal to the surface are expected to be much larger than gradients along the surface, and are therefore assumed to be of order one over delta. These assumed orders of magnitude are applied to each term in the Navier-Stokes equations, and terms of order one are retained.

BOUNDARY LAYER ANALYSES BASIC ASSUMPTIONS

- BOUNDARY LAYER THICKNESS SMALL ($\mathcal{O}(\delta)$)
 - $\rho, u, H, T, \frac{\partial}{\partial x}$ ARE ALL $\mathcal{O}(1)$
 - $\frac{\partial}{\partial y}$ IS $\mathcal{O}\left(\frac{1}{\delta}\right)$
 - KEEP ONLY $\mathcal{O}(1)$ TERMS

BOUNDARY LAYER ANALYSES - BASIC ASSUMPTIONS

Without going through the details of the order-of-magnitude analysis, the next two figures show which terms in the Navier-Stokes equations are eliminated in deriving the boundary layer equations. All second derivatives in the x , or streamwise, direction are eliminated, while second derivatives in the cross-flow direction are retained. In addition, the entire cross-flow momentum equation can be eliminated. This says that, with the boundary layer approximation, the pressure gradient across the boundary layer is negligible.

BOUNDARY LAYER ANALYSES BASIC ASSUMPTIONS

BOUNDARY LAYER ANALYSES BASIC ASSUMPTIONS

$$\frac{\partial(\rho u)}{\partial x} + \frac{\partial(\rho v)}{\partial y} = 0$$

$$\frac{\partial(\rho u^2)}{\partial x} + \frac{\partial(\rho uv)}{\partial y} = -\frac{\partial p}{\partial x} + \frac{1}{Re} \left(\frac{\partial T_{xx}}{\partial x} + \frac{\partial T_{xy}}{\partial y} \right)$$

$$\frac{\partial(\rho v^2)}{\partial x} + \frac{\partial(\rho v^2)}{\partial y} = -\frac{\partial p}{\partial y} + \frac{1}{Re} \left(\frac{\partial T_{xy}}{\partial x} + \frac{\partial T_{yy}}{\partial y} \right)$$

$$\frac{\partial(\rho uH)}{\partial x} + \frac{\partial(\rho vH)}{\partial y} = -\frac{1}{RePr} \left(\frac{\partial q_x}{\partial x} + \frac{\partial q_y}{\partial y} \right) \\ + \frac{1}{Re} \left[\frac{\partial}{\partial x} (uT_{xx} + vT_{xy}) + \frac{\partial}{\partial y} (uT_{xy} + vT_{yy}) \right]$$

$$p = \rho RT$$

$$\tau_{xy} = \mu \left(\frac{\partial u}{\partial x} + \frac{\partial v}{\partial y} \right)$$

$$q_y = -k \frac{\partial T}{\partial y}$$

$$H = c_p T + \frac{1}{2} (u^2 + v^2)$$

7.

BOUNDARY LAYER ANALYSES - GOVERNING EQUATIONS

The resulting boundary layer equations, with the viscous and heat conduction terms expanded, are shown here. Note that the pressure gradient term is written as an ordinary derivative, since pressure is only a function of streamwise location. The pressure is generally assumed to be known, typically from a potential flow or Euler analysis, or from experiment. (In some internal flow applications, the pressure is computed as part of the boundary layer solution using conservation of total mass flow rate as a basis). The boundary layer equations are parabolic in the streamwise direction, and can therefore be solved by marching in the x direction.

BOUNDARY LAYER ANALYSES GOVERNING EQUATIONS

$$\begin{aligned}\frac{\partial(\rho u)}{\partial x} + \frac{\partial(\rho v)}{\partial y} &= 0 \\ \frac{\partial(\rho u^2)}{\partial x} + \frac{\partial(\rho uv)}{\partial y} &= -\frac{dp_e}{dx} + \frac{1}{Re} \frac{\partial}{\partial y} \left(\mu \frac{\partial u}{\partial y} \right) \\ \frac{\partial(\rho u H)}{\partial x} + \frac{\partial(\rho v H)}{\partial y} &= -\frac{1}{Re Pr} \frac{\partial}{\partial y} \left(k \frac{\partial T}{\partial y} \right) + \frac{1}{Re} \frac{\partial}{\partial y} \left(\mu u \frac{\partial u}{\partial y} \right) \\ p &= \rho R T \\ H &= c_p T + \frac{1}{2} u^2 \\ p_e &\text{ KNOWN}\end{aligned}$$

BOUNDARY LAYER ANALYSES - SOLUTION METHODS

The earliest solution methods developed for the boundary layer equations were integral methods. Many different integral methods have been proposed. Typically, they are derived by assuming a functional form for the velocity profile, for instance, a $1/7$ power law, plugging it into the x-momentum equation, and analytically integrating over y . The result is an ordinary differential equation (or in some cases, equations) in x for some boundary layer parameter such as displacement thickness, momentum thickness, etc.

Most of the more recent boundary layer methods solve the partial differential boundary layer equations themselves, by forward marching in the streamwise direction using explicit or implicit finite difference (or finite element) techniques.

BOUNDARY LAYER ANALYSES SOLUTION METHODS

- INTEGRAL METHODS
- EXPLICIT AND IMPLICIT FINITE DIFFERENCE METHODS
- FINITE ELEMENT METHODS

Boundary layer methods are the simplest methods that can be used that include viscous and heat transfer effects. Like potential flow methods, they have been around for a long time. Working computer codes are widely available, and they are generally fairly fast and easy to use.

Although the boundary layer equations include viscous effects, the streamwise viscous diffusion terms have been eliminated. This restricts them to attached flow, so that the streamwise velocity is always positive. (There are, however, various numerical approximations like the "FLARE" approximation (Ref. 9) that allow the equations to be marched through small regions of separated flow). Boundary layer methods are valid only for thin shear layers, and cannot be used to compute completely viscous internal flows. Another disadvantage is the need for a known pressure distribution, requiring an initial potential flow or Euler analysis.

Boundary layer methods are most useful in high Reynolds number flows with thin viscous regions, where the boundary layer has negligible effect on the pressure field. They are generally cheap to use and are therefore often used in preliminary design studies that require many cases to be run. They are sometimes used in conjunction with a potential flow or Euler analysis in an interactive mode. In these cases, typically, the inviscid method is used to get an initial pressure distribution, the boundary layer method is used to get a displacement thickness distribution, a new "effective" body shape is determined, the inviscid method is rerun, etc.

BOUNDARY LAYER ANALYSES

+ 'S AND - 'S

ADVANTAGES

- INCLUDES VISCOUS EFFECTS
- COMPUTER CODES WIDELY AVAILABLE, EASY TO USE
- EQUATIONS ARE PARABOLIC IN x ,
- SOLVED BY STREAMWISE MARCHING

DISADVANTAGES

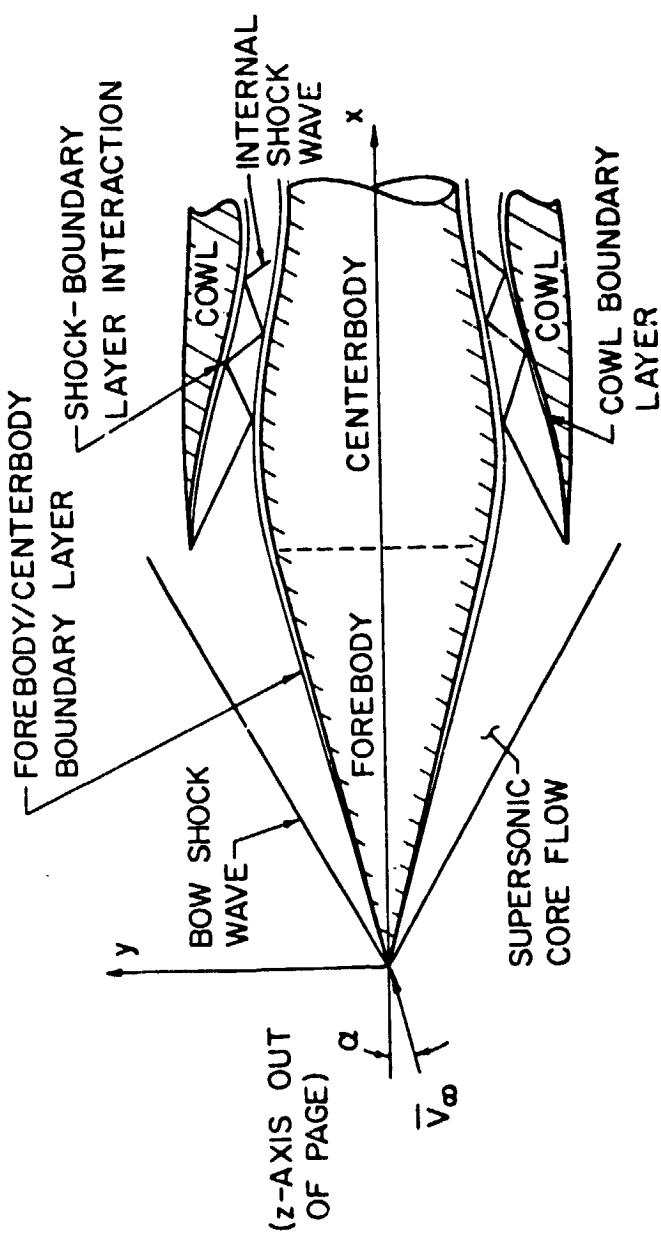
- NO STREAMWISE VISCOUS DIFFUSION
- REQUIRES KNOWN PRESSURE DISTRIBUTION
- ONLY VALID FOR "THIN" SHEAR LAYERS

AREAS OF APPLICATION

- PRELIMINARY DESIGN STUDIES
- VISCOUS/INVISCID INTERACTION
- INLETS, NOZZLES, TURBOMACHINERY

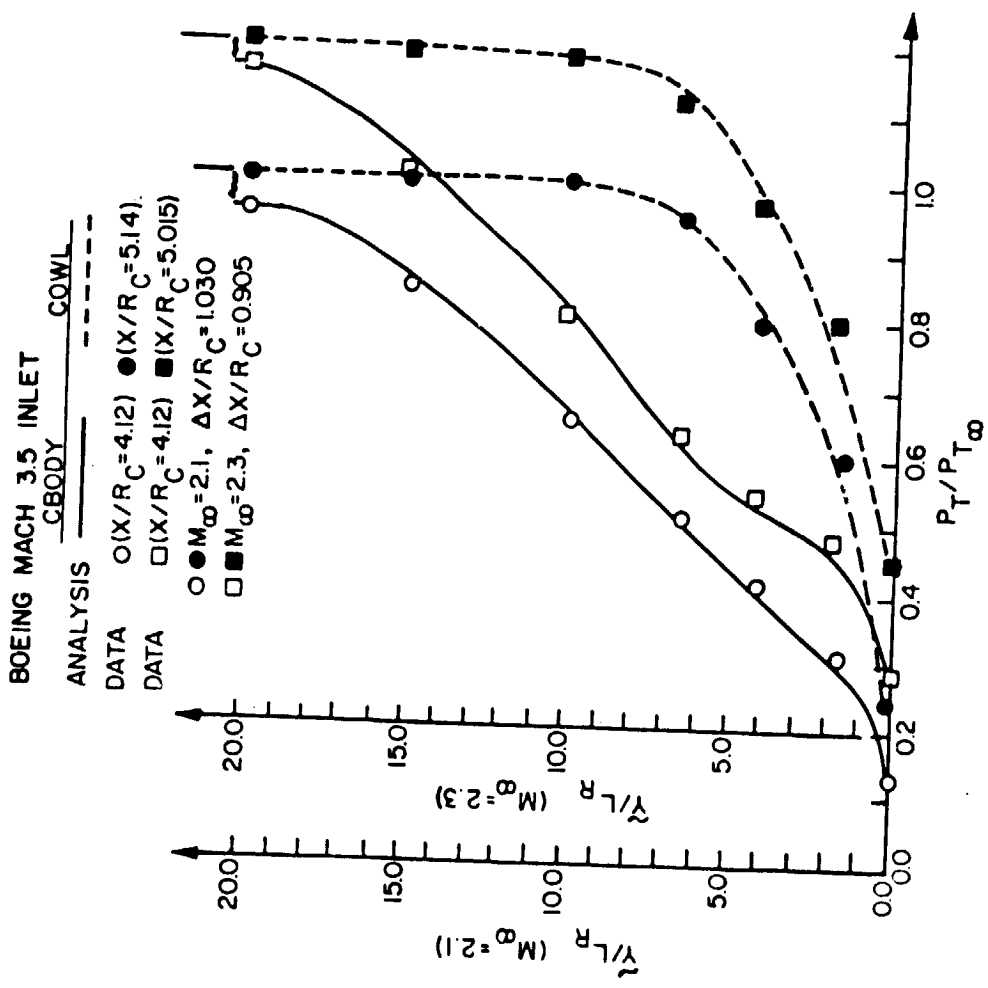
BOUNDARY LAYER ANALYSES - EXAMPLE

As an example of a boundary layer analysis for internal flow, the method of Vadyak, Hoffmann, and Bishop (Ref. 10) for flow through supersonic inlets will be used. This figure is a schematic of a typical mixed-compression supersonic inlet. Boundary layers develop along both the cowl and centerbody. Since there are shock waves in the inlet, shock-boundary layer interactions occur. The method of Reference 10 uses a second-order method of characteristics algorithm with discrete shock wave fitting to compute the inviscid flow through the inlet. The boundary layer is then computed using a second-order implicit finite difference technique, with a control volume analysis for shock-boundary layer interactions.



BOUNDARY LAYER ANALYSES - EXAMPLE

In this figure, computed results from the boundary layer analysis are compared with the experimental data of References 11 and 12 for a Mach 3.5 mixed compression axisymmetric inlet. Total pressure profiles on the cowl and centerbody at the axial stations specified are presented for two different free stream Mach numbers. The effect of viscosity is obvious in the total pressure loss through the boundary layer as the wall is approached. The boundary layer is thicker on the centerbody than the cowl because of its longer development length.



PARABOLIZED NAVIER-STOKES ANALYSES - BASIC ASSUMPTIONS

There are many cases where viscous effects are important, but boundary layer methods are not sufficient. Examples include diffusing internal flows in which boundary layers on opposite walls merge, so that there is no inviscid region, and corner flows, where viscous derivatives in two directions are important. The Navier-Stokes equations could of course be solved for these flows, but they are expensive and often difficult to solve.

Fortunately, for many cases there is an alternative. A reduced set of equations can be derived that are easier to solve than the Navier-Stokes equations, but contain more physics than the boundary layer equations. These are the so-called "parabolized" Navier-Stokes, or PNS, equations, and they are becoming more and more popular. They apply throughout the flow field, which is not split into inviscid and viscous regions. "Parabolized" is actually bad terminology, but it has caught on. The steady flow equations are actually of mixed hyperbolic-parabolic type. The key point, however, is that they can be solved by forward marching in the streamwise direction.

The derivation of the PNS equations is not as rigorous as the boundary layer equations, and several different versions appear in the literature. With some exceptions, the derivation is roughly equivalent to keeping both the order one and order delta terms in the order-of-magnitude analysis used in deriving the boundary layer equations. All methods neglect second derivatives in the streamwise direction. In addition, special treatment is required for the pressure gradient term in the streamwise momentum equation. (More on this later).

PARABOLIZED NAVIER-STOKES ANALYSES BASIC ASSUMPTIONS

- NOT AS RIGOROUS AS DERIVATION OF
BOUNDARY LAYER EQUATIONS
- SEVERAL DIFFERENT VERSIONS ARE USED
- IN GENERAL, NEGLECT STREAMWISE VISCOSUS
DERIVATIVE AND HEAT FLUX TERMS
- SPECIAL TREATMENT OF STREAMWISE VISCOSUS
PRESSURE GRADIENT IN SUBSONIC REGIONS
- ROUGHLY EQUIVALENT TO KEEPING $\theta(1)$ AND $\theta(\delta)$
TERMS IN BOUNDARY LAYER DERIVATION

PARABOLIZED NAVIER-STOKES ANALYSES - BASIC ASSUMPTIONS

This figure indicates the terms eliminated from the Navier-Stokes equations in deriving one version of the PNS equations. Derivatives in the streamwise direction in the viscous and heat conduction terms are eliminated. Note that, unlike in the boundary layer equations, the cross-flow momentum equation is retained in the PNS equations.

PARABOLIZED NAVIER-STOKES ANALYSES BASIC ASSUMPTIONS

PARABOLIZED NAVIER-STOKES ANALYSES BASIC ASSUMPTIONS

$$\begin{aligned}
 \frac{\partial(\rho u)}{\partial x} + \frac{\partial(\rho v)}{\partial y} &= 0 \\
 \frac{\partial(\rho u^2)}{\partial x} + \frac{\partial(\rho uv)}{\partial y} &= -\frac{\partial p}{\partial x} + \frac{1}{Re} \left(\frac{\partial \tau_{xz}}{\partial x} + \frac{\partial \tau_{xy}}{\partial y} \right) \\
 \frac{\partial(\rho uv)}{\partial x} + \frac{\partial(\rho v^2)}{\partial y} &= -\frac{\partial p}{\partial y} + \frac{1}{Re} \left(\frac{\partial \tau_{zy}}{\partial x} + \frac{\partial \tau_{yy}}{\partial y} \right) \\
 \frac{\partial(\rho uH)}{\partial x} + \frac{\partial(\rho vH)}{\partial y} &= -\frac{1}{RePr} \left(\frac{\partial q_x}{\partial x} + \frac{\partial q_y}{\partial y} \right) \\
 &\quad + \frac{1}{Re} \left[\frac{\partial}{\partial x} (u \tau_{xz} + v \tau_{xy}) + \frac{\partial}{\partial y} (u \tau_{xy} + v \tau_{yy}) \right] \\
 p &= \rho R T \\
 \tau_{xy} &= \mu \left(\frac{\partial y}{\partial x} + \frac{\partial u}{\partial y} \right) \\
 \tau_{yy} &= 2\mu \frac{\partial v}{\partial y} + \lambda \left(\frac{\partial y}{\partial x} + \frac{\partial v}{\partial y} \right) \\
 q_y &= -k \frac{\partial T}{\partial y} \\
 H &= c_p T + \frac{1}{2}(u^2 + v^2)
 \end{aligned}$$

PARABOLIZED NAVIER-STOKES ANALYSES - GOVERNING EQUATIONS

The resulting PNS equations are shown here, with the viscous and heat conduction terms expanded. Except for the pressure gradient term in the x-momentum equation, these equations are of mixed hyperbolic-parabolic type in the x, or streamwise, direction, and can be solved by forward marching in x. However, the pressure gradient term makes the streamwise momentum equation elliptic in the x direction, for subsonic flow. This occurs not only in completely subsonic flow, but also in the subsonic region near the wall in primarily supersonic flow. Various procedures have been used to handle these cases and still allow a streamwise marching solution procedure. The way the streamwise pressure gradient is treated is often what distinguishes one PNS method from another.

As presented here, the equations are for two-dimensional flow. However, PNS analyses are also used, perhaps even more often, for three-dimensional flow.

PARABOLIZED NAVIER-STOKES ANALYSES GOVERNING EQUATIONS

$$\begin{aligned}\frac{\partial(\rho u)}{\partial x} + \frac{\partial(\rho v)}{\partial y} &= 0 \\ \frac{\partial(\rho u^2)}{\partial x} + \frac{\partial(\rho uv)}{\partial y} &= -\frac{\partial p}{\partial x} + \frac{1}{Re} \frac{\partial}{\partial y} \left(\mu \frac{\partial u}{\partial y} \right) \\ \frac{\partial(\rho uv)}{\partial x} + \frac{\partial(\rho v^2)}{\partial y} &= -\frac{\partial p}{\partial y} + \frac{1}{Re} \frac{\partial}{\partial y} \left[(2\mu + \lambda) \frac{\partial u}{\partial y} \right] \\ \frac{\partial(\rho uH)}{\partial x} + \frac{\partial(\rho vH)}{\partial y} &= -\frac{1}{RePr} \frac{\partial}{\partial y} \left(k \frac{\partial T}{\partial y} \right) \\ &\quad + \frac{1}{Re} \frac{\partial}{\partial y} \left[\mu u \frac{\partial v}{\partial y} + (2\mu + \lambda)v \frac{\partial u}{\partial y} \right]\end{aligned}$$

$$P = \rho RT$$

$$H = C_v T + \frac{1}{2} (u^2 + v^2)$$

PARABOLIZED NAVIER-STOKES ANALYSES - SOLUTION METHODS

In solving the PNS equations, finite difference methods dominate, although finite element methods have some strong advocates. As mentioned previously for Euler analyses, the trend is towards the use of implicit instead of explicit methods.

PARABOLIZED NAVIER-STOKES ANALYSES SOLUTION METHODS

- EXPLICIT AND IMPLICIT FINITE DIFFERENCE METHODS
- FINITE ELEMENT METHODS

PARABOLIZED NAVIER-STOKES ANALYSES - +'S AND -'S

Since the PNS equations include the cross-flow momentum equations, and retain viscous derivatives in both cross-flow directions (in 3-D), they apply to flow situations that boundary layer methods can't handle. They are used throughout the flow field, so a separate inviscid solution may not be needed. And, since the equations are solved by spatial marching, PNS methods are faster and use less storage than Navier-Stokes methods.

As in boundary layer analyses, however, neglecting the streamwise viscous diffusion terms means the flow must remain attached (except for small separation bubbles that can be computed using the "FLARE" approximation). A final problem with PNS methods is that they are still somewhat "researchy" and can be difficult to use, especially for complex geometries.

PNS methods are most applicable to relatively high Reynolds number flows without reverse flow. They are at the stage where they can be used in design, but are generally used more for verification and problem investigation than for large parametric studies.

PARABOLIZED NAVIER-STOKES ANALYSES +'S AND -'S

ADVANTAGES

- INCLUDES CROSS-FLOW MOMENTUM EQUATIONS
- VALID FOR FULLY VISCOUS FLOW
- EQUATIONS SOLVED BY STREAMWISE MARCHING

DISADVANTAGES

- NO STREAMWISE VISCOUS DIFFUSION
- COMPUTER CODES CAN BE DIFFICULT TO USE

AREAS OF APPLICATION

- DESIGN VERIFICATION
- FLOW PHYSICS INVESTIGATIONS
- INLETS, DIFFUSERS, NOZZLES, TURBOMACHINERY

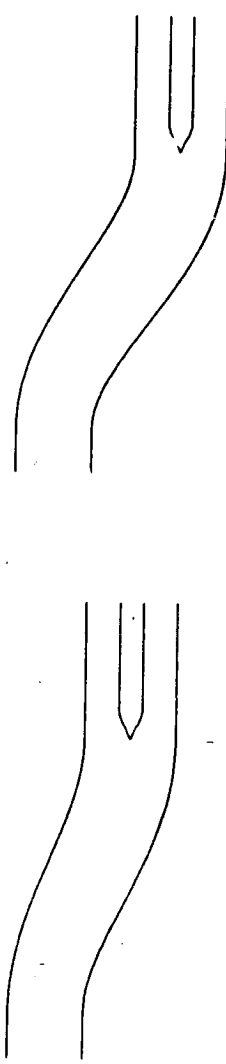
PARABOLIZED NAVIER-STOKES ANALYSES - EXAMPLE 1

This example will show results from a three-dimensional parabolized Navier-Stokes analysis for subsonic flow. The computations were done by Towne and Flitcroft as part of a joint NASA/RAE research program on intake duct flows (Ref. 13). Using the method of References 14-16, PNS calculations were made for flow through two generic S-shaped intake ducts, as shown in this figure. Both intake ducts had circular cross-sections and an area ratio of 1.4. The flow was turbulent, with inlet Mach numbers that ranged from 0.395 to 0.794 and Reynolds numbers (based on inlet diameter and flow conditions) from 3.9 to 6.6 million.

Lewis Research Center

NASA

RAE2129 INTAKE DUCTS



OFFSET/LENGTH = 0.30

OFFSET/LENGTH = 0.45

- Area Ratio = 1.4
- Inlet Mach Number = 0.395 to 0.794
- Reynolds Number = 3.9 to 6.6 million
- Inlet Boundary Layer = 0.06D

59

PARABOLIZED NAVIER-STOKES ANALYSES - EXAMPLE 1

In this figure, the development of pressure-driven secondary flow is shown for the 0.45 offset S-duct. Computed secondary velocity vectors (i.e., the velocity in planes normal to the duct centerline) are presented at three streamwise stations. In the first bend, the high pressure at the outside of the bend drives the low energy boundary layer toward the inside, while the core flow responds to centrifugal effects and moves toward the outside. The result is a pair of counter-rotating secondary flow vortices.

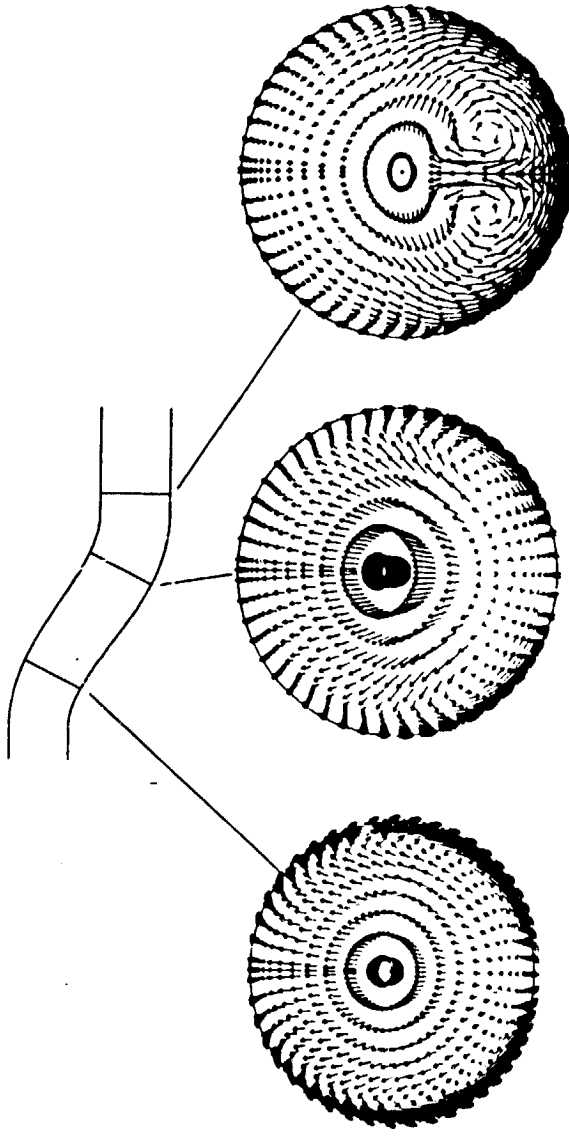
In the second bend, the direction of the cross-flow pressure gradients reverses. However, the flow enters the second bend with a vortex pattern already established. The net effect is to tighten and concentrate these vortices near the bottom of the duct, in agreement with classical secondary flow theory.

National Aeronautics and
Space Administration
Lewis Research Center

COMPUTATIONAL METHODS BRANCH



RAE 2129 S-DUCT
Secondary Flow Development



PARABOLIZED NAVIER-STOKES ANALYSES - EXAMPLE 1

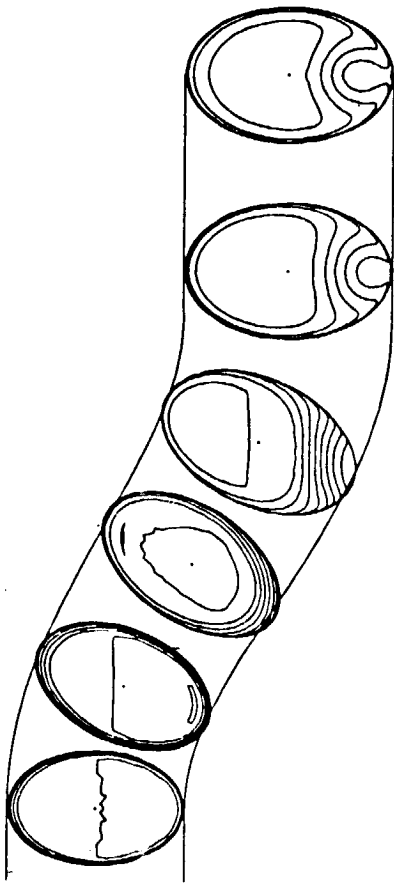
The secondary flows that are set up in the S-duct cause a significant amount of flow distortion. In this figure, contours of constant streamwise velocity (i.e., the velocity in the direction of the duct centerline) are shown at several stations. As the flow enters the first bend, the boundary layer at the top of the duct initially thickens due to the locally adverse pressure gradient in that region. The effects of the secondary flow soon dominate, however, and by the end of the duct most of the low-energy flow has moved to the bottom of the duct. This horseshoe-shaped distortion pattern is typical of S-bend flows.

National Aeronautics and
Space Administration
Lewis Research Center



COMPUTATIONAL METHODS BRANCH

RAE 2129 S-DUCT
Offset/Length = 0.30, No Hub, $M = 0.608$



21

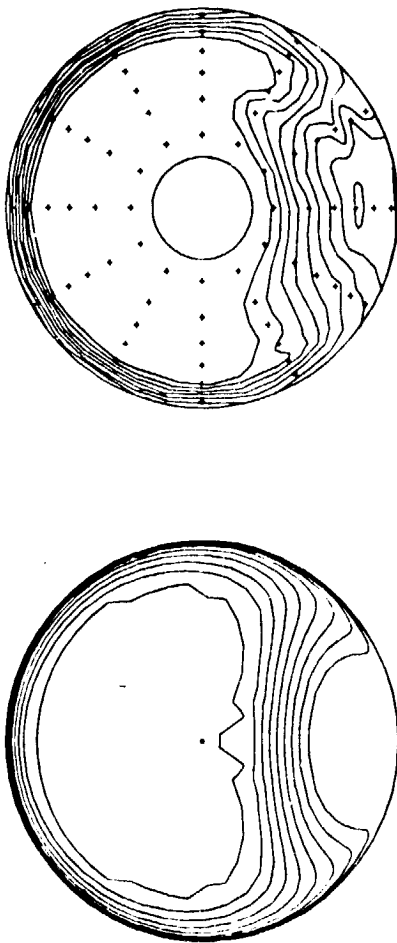
PARABOLIZED NAVIER-STOKES ANALYSES - EXAMPLE 1

In this figure, computed total pressure contours at the duct exit are compared with experimental data for the same duct from Reference 17. The agreement is very good. This case used a $50 \times 50 \times 67$ mesh, and required 7 minutes of CPU time on a Cray XMP computer system.

Lewis Research Center

NASA

COMPRESSOR FACE TOTAL PRESSURE
Offset/Length = 0.30, No Hub, $M = 0.608$



22.

PARABOLIZED NAVIER-STOKES ANALYSES - EXAMPLE 2

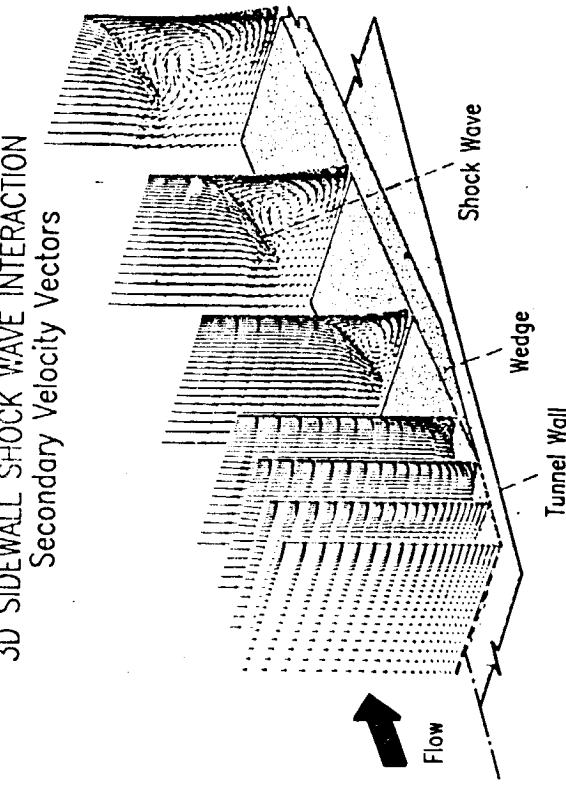
In this figure, computed results are presented from a three-dimensional parabolized Navier-Stokes analysis for supersonic flow. The analysis was done by Anderson and Benson (Ref. 18) using the method of References 19 and 20. The problem is a three-dimensional sidewall shock - boundary layer interaction. Complex interactions like this often occur in "two-dimensional" mixed-compression supersonic inlets. The shock is generated by a ten degree wedge mounted in a wind tunnel, flush with the sidewall. The incoming Mach number is 2.94.

Shown in the figure are the secondary velocity vectors (i.e., the velocity vectors in the cross-flow directions, without the streamwise component) at selected streamwise stations. The shock position is indicated by the change in direction of the secondary velocity vectors. The high pressure downstream of the shock (which is the region nearest the wedge surface) forces the low-energy boundary layer flow to migrate upward along the sidewall. The flow on the wedge is then drawn in toward the sidewall and the flow moving up the sidewall turns over, forming a complex secondary flow vortex in the corner. The low energy flow thus accumulates in the corner region, and is probably the cause of the high heating rates detected experimentally (Ref. 21).

NASA

Computational Methods Branch

3D SIDEWALL SHOCK WAVE INTERACTION
Secondary Velocity Vectors



NASA

Lewis Research Center

NAVIER-STOKES ANALYSES - GOVERNING EQUATIONS

These equations are the same as those shown at the beginning of this presentation. The term "time-averaged" refers to the procedure used to develop equations for turbulent flow that can be solved for practical problems with today's computer systems. They can still be used for unsteady turbulent flow, as long as the time scale of the unsteadiness is long compared to the time scale of the turbulent fluctuations. For laminar flow these equations are exact, and involve no assumptions or approximations. For turbulent flow the only assumption (and depending on the complexity of the flow, it could be a big one) is in the choice of turbulence model. For unsteady flow, the Navier-Stokes equations are of mixed hyperbolic-parabolic type.

TIME-AVERAGED NAVIER-STOKES ANALYSES GOVERNING EQUATIONS

$$\frac{\partial \rho}{\partial t} + \frac{\partial(\rho u)}{\partial x} + \frac{\partial(\rho v)}{\partial y} = 0$$

$$\frac{\partial(\rho u)}{\partial t} + \frac{\partial(\rho u^2)}{\partial x} + \frac{\partial(\rho uv)}{\partial y} = -\frac{\partial p}{\partial x} + \frac{1}{Re} \left(\frac{\partial \tau_{xx}}{\partial x} + \frac{\partial \tau_{xy}}{\partial y} \right)$$

$$\frac{\partial(\rho v)}{\partial t} + \frac{\partial(\rho uv)}{\partial x} + \frac{\partial(\rho v^2)}{\partial y} = -\frac{\partial p}{\partial y} + \frac{1}{Re} \left(\frac{\partial \tau_{xy}}{\partial x} + \frac{\partial \tau_{yy}}{\partial y} \right)$$

$$\begin{aligned} \frac{\partial(\rho E_r)}{\partial t} + \frac{\partial(uE_r)}{\partial x} + \frac{\partial(vE_r)}{\partial y} &= -\frac{\partial(vp)}{\partial x} - \frac{\partial(vp)}{\partial y} - \frac{1}{RePr} \left(\frac{\partial q_x}{\partial x} + \frac{\partial q_y}{\partial y} \right) \\ &+ \frac{1}{Re} \left[\frac{\partial}{\partial x} (u\tau_{xx} + v\tau_{xy}) + \frac{\partial}{\partial y} (u\tau_{xy} + v\tau_{yy}) \right] \end{aligned}$$

TIME-AVERAGED NAVIER-STOKES ANALYSES AUXILIARY EQUATIONS

$$P = \rho RT$$

$$\begin{aligned} \tau_{xx} &= 2\mu \frac{\partial u}{\partial x} + \lambda \left(\frac{\partial u}{\partial x} + \frac{\partial v}{\partial y} \right) \\ \tau_{yy} &= 2\mu \frac{\partial v}{\partial y} + \lambda \left(\frac{\partial u}{\partial x} + \frac{\partial v}{\partial y} \right) \\ \tau_{xy} &= \mu \left(\frac{\partial v}{\partial x} + \frac{\partial u}{\partial y} \right) \end{aligned}$$

$$\begin{aligned} q_x &= -k \frac{\partial T}{\partial x} \\ q_y &= -k \frac{\partial T}{\partial y} \end{aligned}$$

$$E_T = \rho c_v T + \frac{1}{2} \rho (u^2 + v^2)$$

NAVIER-STOKES ANALYSES - SOLUTION METHODS

The Navier-Stokes equations are usually solved by marching in time. As with the unsteady Euler equations, if only the steady state solution is of interest, acceleration techniques are often used to speed convergence, and the results may not be time accurate. Both explicit and implicit methods have been used, with the trend today toward implicit methods.

TIME-AVERAGED NAVIER-STOKES ANALYSES SOLUTION METHODS

- EXPLICIT AND IMPLICIT FINITE DIFFERENCE METHODS
- FINITE ELEMENT METHODS

NAVIER-STOKES ANALYSES - +'S AND -'S

Except for the need to model (instead of actually compute) turbulence, the Navier-Stokes equations are the most complete mathematical model possible for continuum flow of a Newtonian fluid. No other assumptions or approximations are built into the governing equations. However, various assumptions, such as a perfect gas law, are often used in the auxiliary equations.

Unfortunately, using a Navier-Stokes method is expensive. They are also newer and less mature than simpler methods. Developing and/or using a Navier-Stokes analysis is not necessarily straightforward, and is basically still a research area itself.

The Navier-Stokes equations can be applied to any type of flow. The expense and difficulty involved in using them currently limits their practical application. They can be used in design problems where the potential payoff is high enough to offset their cost, and in research into complex flow physics problems.

TIME-AVERAGED NAVIER-STOKES ANALYSES +'S AND -'S

ADVANTAGES

- MOST COMPLETE FLOW MODEL POSSIBLE
(EXCEPT FOR TURBULENCE MODELING)

DISADVANTAGES

- EXPENSIVE (IN CPU TIME, MEMORY, \$)
- COMPUTER CODES CAN BE DIFFICULT TO USE

AREAS OF APPLICATION

- DESIGN VERIFICATION
- FLOW PHYSICS INVESTIGATIONS
- INLETS, DIFFUSERS, NOZZLES, TURBOMACHINERY

TIME-AVERAGED NAVIER-STOKES ANALYSES - EXAMPLE

This figure compares results from a two-dimensional time-averaged Navier-Stokes analysis with experimental data for a normal shock - boundary layer interaction. This type of interaction occurs in the throat region of a mixed or internal compression supersonic inlet. The analysis was performed by Benson at NASA Lewis using the implicit finite difference method of Reference 22, and the experiment was done by Hingst, also at NASA Lewis, using laser-Doppler velocimetry. The analysis used a computational grid of 60 axial by 40 normal points. The points in the normal direction were packed near the wall to resolve the boundary layer, but no packing was done in the axial direction.

The Navier-Stokes analysis duplicated all the important physical phenomena in the experiment. Although difficult to see in this type of plot, both shocks had a lambda shape near the boundary layer. The influence of the shock feeds upstream through the subsonic part of the boundary layer, an effect not present in boundary layer or parabolized Navier-Stokes analyses. Note that, as in any shock capturing method, the shock is smeared in the axial direction in the analytical results. The shock could be made sharper by using more mesh points and/or packing points near the shock. The boundary layer downstream of the shock is somewhat thicker in the analysis than the experiment, probably due to inadequate mesh resolution.

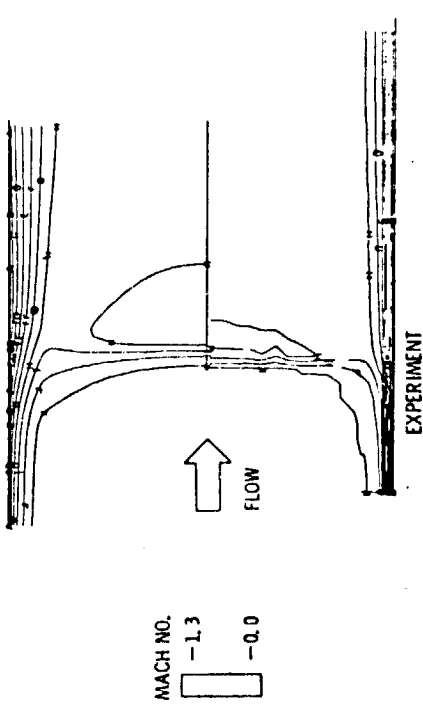
National Aeronautics and
Space Administration
Lewis Research Center

COMPUTATIONAL METHODS BRANCH

NASA

MACH 1.3 NORMAL SHOCK WAVE BOUNDARY LAYER INTERACTION

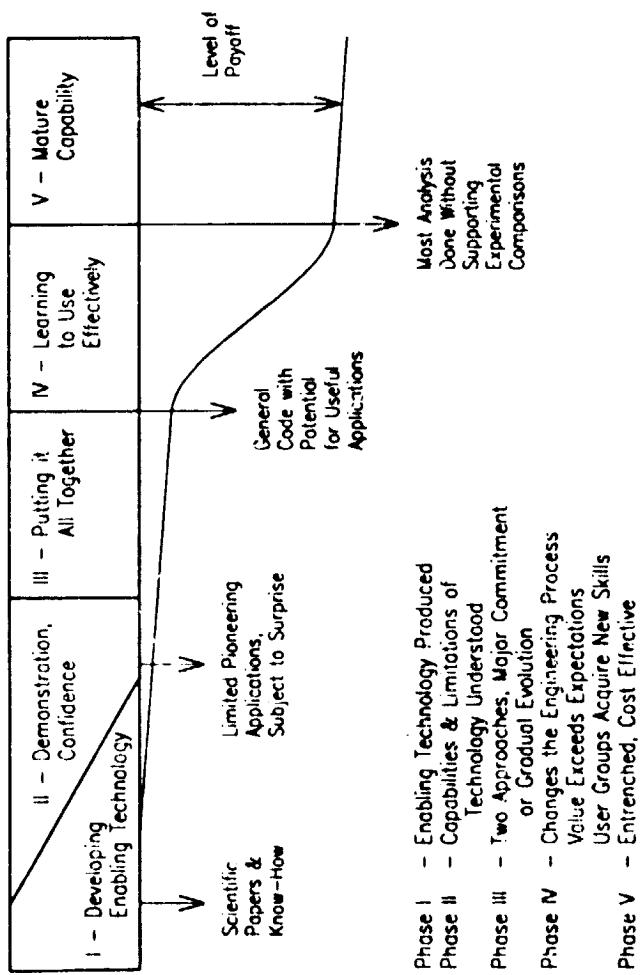
COMPARISON OF LDV EXPERIMENT AND ANALYSIS



CFD DEVELOPMENT STAGES

Recently, a survey of current capabilities and future directions in computational fluid dynamics was conducted by a committee of the National Research Council's Aeronautics and Space Engineering Board (Ref. 21). The next three figures summarize the results of that survey as they relate to internal flows. The committee divided the CFD development cycle into five stages, from the beginning development of the necessary technology through the availability of a mature predictive capability. This cycle could apply to a general type of analysis, or to a specific individual computer code.

CFD DEVELOPMENT STAGES



STATUS OF CFD IN PROPULSION

The committee surveyed CFD developers and users nationwide. This figure summarizes the results for the status of CFD in propulsion. The status of different types of analyses, listed in the first column, are shown for different types of propulsion system components, listed across the top row. The term "stationary" refers to inlets, nacelles, diffusers, and nozzles, while "rotating" refers to fans, compressors, turbines, propellers, and rotors. The numbers in the table correspond to stages in the development cycle shown in the previous figure.

In general, simpler methods are further along in development than more complex methods, and two-dimensional versions are further along than three-dimensional versions. Unsteady analyses are generally weak overall.

STATUS OF CFD IN PROPULSION

Flow Complexity Governing Equations	Stationary			Rotating			Combustors
	2-D	3-D	Unsteady	2-D	3-D	Unsteady	
INVSCID							
Full Potential	5.0	4.0		4.5	4.0	0.5	
Euler	4.5	3.5	3.0	4.0	2.5	1.5	
VISCUS							
Transitional / Turbulent	4.5	3.0	1.5	4.0	2.5	1.0	
Boundary Layer							
Parabolized	4.5	3.5	1.0	4.0	2.5	0.5	
Navier-Stokes							
Viscous-inviscid	3.5	1.0	0.5	2.5	0.5	0.5	
Interaction							
Time Averaged	3.5	2.5	1.5	2.5	1.0	0.5	
Navier-Stokes							
							2.0

KEY

- 1 - Evolving enabling technology
- 2 - Understanding capabilities & limitations
- 3 - Beginning to apply
- 4 - Learning to use effectively
- 5 - Mature capability

STATUS OF CFD IN PROPULSION - PROBLEM AREAS

The previous figure gave a summary of the general overall status of CFD in propulsion. However, current CFD codes are inadequate in several specific areas. Some important ones are listed here. Some of these are related to the computation of various flow phenomena important in propulsion systems, and some are related to the use of CFD codes in general.

STATUS OF CFD IN PROPULSION PROBLEM AREAS

- 3-D SHOCK-BOUNDARY LAYER INTERACTION
- FLOW SEPARATION
- LARGE AMOUNTS OF BLEED
- HEAT TRANSFER W/WO FILM COOLING
- TOTAL PRESSURE LOSS
- UNSTEADY FLOWS
- COMPLEX GEOMETRIES
- TURBULENCE AND TRANSITION MODELING
- COMPONENT COUPLING
- BENCHMARK DATA FOR CODE VERIFICATION:
- "KNOBS AND SWITCHES"
- COMPUTER RESOURCES REQUIRED

REFERENCES - SPECIFIC

1. Kao, H. C., "Some Aspects of Calculating Flows About Three-Dimensional Subsonic Inlets," NASA TM 82678, 1981.
2. Hess, J. L., Mack, D. P., and Stockman, N. O., "An Efficient User-Oriented Method for Calculating Compressible Flow In and About Three-Dimensional Inlets," NASA CR 159578, April 1979.
3. Lieblein, S., and Stockman, N. O., "Compressibility Correction for Internal Flow Solutions," Journal of Aircraft, Vol. 9, No. 4, April 1972, pp. 312-313.
4. Abbot, J. M., "Aerodynamic Performance of a Scoop Inlet," NASA TM 73725, 1977.
5. Reyhner, T. A., "Computation of Transonic Potential Flow About Three-Dimensional Inlets, Ducts, and Bodies," NASA CR 3514, March 1982.
6. Chima, R. V., and Johnson, G. M., "Efficient Solution of the Euler and Navier-Stokes Equations with a Vectorized Multiple-Grid Algorithm," AIAA Journal, Vol. 23, No. 1, Jan. 1985, pp. 23-32.
7. Chima, R. V., "Development of an Explicit Multigrid Algorithm for Quasi-Three-Dimensional Viscous Flows in Turbomachinery," NASA TM 87228, 1986.
8. McFarland, E. R., "A Rapid Bla-e-to-BL² Solution for Use in Turbomachinery Design," Journal of Engineering for Gas Turbines and Power, Vol. 106, No. 2, April 1984, pp. 376-382.
9. Reyhner, T. A., and Flugge-Lotz, I., "The Interaction of a Shock Wave with a Laminar Boundary Layer," International Journal of Non-Linear Mechanics, Vol. 3, 1968, pp. 173-199.
10. Vadyak, J., Hoffman, J. D., and Bishop, A. R., "Three-Dimensional Flow Simulations for Supersonic Mixed-Compression Inlets at Incidence," AIAA Journal, Vol. 22, No. 7, July 1984, pp. 873-881.
11. Syberg, J. S., and Koncsek, J. L., "Experimental Evaluation of a Mach 3.5 Axisymmetric Inlet," NASA CR 2563, 1975.
12. Koncsek, J. L., "Machine Plot Supplement to D6-42494," Rept. D6-42595, The Boeing Company, Seattle, Wash., 1975.
13. Towne, C. E., and Flitcroft, J. E., "Analysis of Intake Ducts Using a Three-Dimensional Viscous Marching Procedure," Presented at the First World Congress on Computational Mechanics, The University of Texas at Austin, Sept. 22-26, 1986.
14. Briley, W. R., and McDonald, H., "Analysis and Computation of Viscous Subsonic Primary and Secondary Flows," AIAA Paper 79-1453, July 1979.

15. Levy, R., McDonald, H., Briley, W. R., and Kreskovsky, J. P., "A Three-Dimensional Turbulent Compressible Subsonic Duct Flow Analysis for Use with Constructed Coordinate Systems," AIAA Paper 80-1398, July 1980.
16. Levy, R., Briley, W. R., and McDonald, H., "Viscous Primary/Secondary Flow Analysis for Use with Nonorthogonal Coordinate Systems," AIAA Paper 83-0556, Jan. 1983.
17. Willmer, A. C., Brown, T. W., and Goldsmith, E. L., "Effects of Intake Geometry on Circular Pitot Intake Performance at Zero and Low Forward Speeds," Aerodynamics of Power Plant Installation, AGARD CP 301, Paper No. 5, May 1981.
18. Anderson, B. H., and Benson, T. J., "Numerical Solution to the Glancing Sidewall Oblique Shock Wave/Turbulent Boundary Layer Interaction in Three Dimension," AIAA Paper 83-0136, Jan. 1983 (also NASA TM 83056, 1983).
19. Biegel, R. C., McDonald, H., Kreskovsky, J. P., and Levy, R., "Development of a Three-Dimensional Supersonic Inlet Flow Analysis," NASA CR 3218, Nov. 1979.
20. Biegel, R. C., McDonald, H., and Kim, Y.-N., "Computation of Multi-Dimensional Viscous Supersonic Flow by Spatial Forward Marching," AIAA Paper 83-0177, Jan. 1983.
21. Oskam, B., Vas, I. E., and Bogdonoff, S. M., "Mach 3.0 Oblique Shock Wave/Turbulent Boundary Layer Interactions in Three Dimensions," AIAA Paper 76-336.
22. Liu, N.-S., Shamroth, S. J., and McDonald, H., "Numerical Solutions of Navier-Stokes Equations for Compressible Turbulent Two/Three Dimensional Flows in the Terminal Shock Region of an Inlet/Diffuser," NASA CR 3723, Aug. 1983.
23. National Research Council, Current Capabilities and Future Directions in Computational Fluid Dynamics, National Academy Press, 1986.

REFERENCES - GENERAL

- Anderson, D. A., Tannehill, J. C., and Fletcher, R. H., Computational Fluid Mechanics and Heat Transfer, Hemisphere Publishing Corporation, McGraw-Hill Book Company, 1984.
- Zucrow, M. J., and Hoffman, J. D., Gas Dynamics, Volumes 1 and 2, John Wiley & Sons, Inc., 1976.
- Cebeci, T., and Smith, A. M. O., Analysis of Turbulent Boundary Layers, Academic Press, 1974.
- Murthy, S. N. B., and Paynter, G. C., eds., Numerical Methods for Engine-Airframe Integration, Progress in Astronautics and Aeronautics, Vol. 102, AIAA, 1986.